The role of competing magnetic interactions on the abnormal expansion properties in manganese antiperovskites, $Mn_{3+x}A_{1-x}N$ (A = Ni, Sn)

David Boldrin[a,*], Lesley Cohen[a]

[a]*Department of Physics, Blackett Laboratory, Imperial College London, London, SW7 2AZ, United Kingdom*

Abstract

The role of competing magnetic interactions in Mn-doped manganese antiperovskites $Mn_{3+x}A_{1-x}N$ (A = Ni and Sn) has been explored using magnetometry and dilatometry, with particular focus on their relation to abnormal expansion properties. Rare negative magnetisation phenomena are found in zero-field-cooled conditions for both A = Sn and Ni when Mn is doped on the A site. Such behaviour is evidence of both competing magnetic sublattices and magnetocrystalline anisotropy. By comparison with other compounds with the antiferromagnetic Γ_{5g} magnetic structure, we suggest that competing interactions along with magneto-volume coupling influence the near-zero thermal expansion behaviour at intermediate temperatures below T_N in the A = Ni family.

Keywords: `magneto-volume effects; nitride materials; magnetically ordered materials`
2010 MSC: 00-01, 99-00

1. Introduction

Manganese nitride antiperovskites, Mn_3AN (A = Ni, Sn, Ga, Cu, Ag), have recently attracted much attention due to their strong magnetostructural coupling which leads to a range of fascinating properties such as anomalous thermal expansion, abnormal magnetoresistance, barocaloric, baromagnetic and piezomagnetic effects [1–6]. The origin of these properties lies in an unusual combination of electronic features: firstly, a sharp singularity in the density of states due to a narrow Mn_d–N_p band [7], quite common in itinerant ferromagnets, and secondly, a noncollinear antiferromagnetic order born from frustrated Mn–Mn magnetic interactions. The formers influence on the latter induces instabilities in both nuclear and magnetic structures, hence leading to strong magnetostructural correlations.

The flexibility of the manganese antiperovskite nitride structure, which originates from Mn_4N, allows the A site to take many different atoms and also be partially occupied by both A and Mn. Therefore, a more accurate formula is $Mn_{3+x}A_{1-x}N$. One of the most studied members of this family is Mn_3GaN as it combines a large magnetovolume coupling (MVC) with a first-order antiferromagnetic transition at $T_N \sim 300$ K [1, 8]. Consequently, at T_N a concomitant volume change of $\Delta L/L \sim 2\,\%$ is found. Below T_N, the Mn moments adopt the noncollinear antiferromagnetic structure, termed Γ_{5g} (Figure 1a inset), whilst cubic crystallographic symmetry is maintained. A similarly large magnetovolume change at T_N (160K) is found in Mn_3ZnN along with a transition to the Γ_{5g} magnetic structure [1, 9]. As such, it is argued that maintaining the Γ_{5g} structure below T_N is of crucial importance for achieving desirably large magnetostructural properties.

In this paper we report on the magnetic properties of two members of the antiperovskite family $Mn_{3+x}A_{1-x}N$ with A = Ni and Sn and $0 \leq x \leq 0.5$. Both share the same Γ_{5g} magnetic structure of Mn_3GaN, although with additional magnetic phases existing in certain temperature regimes [8–10], and are therefore of interest for their magnetic properties. For A = Ni, when $x = 0$ a similar MVC to the A = Ga member is found [11]. The

☆Fully documented templates are available in the elsarticle package on CTAN.

*Corresponding author
Email address: `d.boldrin@imperial.ac.uk` (Lesley Cohen)

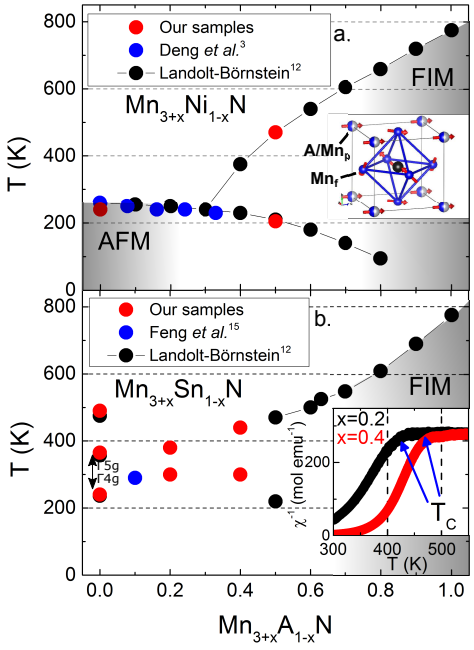

Figure 1: Magnetic phase diagrams as a function of Mn doping on the A site of $Mn_{3+x}A_{1-x}N$ for **a.** A = Ni and **b.** A = Sn. **a. inset** Non-collinear antiferromagnetic Γ_{5g} structure for $Mn_{3+x}A_{1-x}N$ ($x > 0$) with Mn_f the solely occupied Mn site and Mn_p the A site with Mn doping at $x > 0$. **b. inset** Inverse susceptibility of $Mn_{3.8}Sn_{0.2}N$ and $Mn_{3.6}Sn_{0.4}N$ showing the transition temperature from paramagnetism to magnetic order.

phase diagram when $x > 0$ is well explored and a recent study has found a broad region of near-zero thermal expansion (ZTE), *i.e.* Invar-like behaviour, below T_N for $x = 0.33$ [3]. As shown in the phase diagram of Figure 1a, when $x > 0.4$ a second transition occurs at temperatures higher than T_N to a ferromagnetic-like state due to the additional contribution from the excess Mn [12]. For A = Sn and $x = 0$ a transition to the Γ_{5g} magnetic structure occurs at $T \sim 380$ K although it is not associated with any MVC [13]. When $x = 0.5$, an additional high magnetisation state is introduced [14], however the phase diagram between $0 < x < 0.5$ is relatively unexplored (Figure 1b) save for a single study at $x = 0.1$ which reported a magnetic transition at room temperature and weak ferro- (FM) or ferrimagnetism (FIM) [15]. Excess Mn-doping of these antiperovskites often leads to drastic changes in their magnetic properties, such as spin-glass states and transitions involving large changes in magnetisation [16, 17]. Given the many interesting properties of the $Mn_{3+x}A_{1-x}N$ family and their potential utility in a variety of fields, we were motivated to compare the magnetic and thermal properties of two $Mn_{3+x}A_{1-x}N$ systems with $x \geq 0$, which share similar magnetic ordering but have differing magnitude of MVC. This comparison provides important insight into the influence that competing magnetic interactions have on the appearance of near-ZTE at intermediate temperatures below T_N in these materials.

2. Experimental

Samples were prepared using a standard solid state synthesis technique. Firstly, $Mn_2N_{0.86}$ was formed by reacting elemental Mn powder (VWR, 325 mesh, 99.95 %) under dry, flowing nitrogen gas at 700°C for 48 hours. The refined lattice parameters of the $Mn_2N_{0.86}$ indicated this was the correct stoichiometry, rather than stoichiometric Mn_2N. Subsequently, the $Mn_2N_{0.86}$ precursor was ball-milled and then thoroughly mixed by hand with elemental Ni (Sigma Aldrich, $< 150\,\mu$m, 99.99 %) or Sn powder (Alfa-Aesar, -100 mesh, 99.86 %). The resulting mixture was pressed into ~ 2 g pellets, wrapped in Ta foil and sealed in evacuated quartz ampoules. The ampoules were heated to 780°C for 3 days before being quenched to room temperature in water, which was found to improve the crystallinity of the final product, particularly for the A = Sn compounds. For A = Ni and Sn samples were prepared with $x = 0, 0.5$ and $x = 0, 0.2$ and 0.4, respectively, according to the formula $Mn_{3+x}A_{1-x}N$.

X-ray diffraction measurements were performed on a Bruker D2 Phaser diffractometer in Bragg-Brentano geometry with Cu kα radiation (λ = 1.5418 Å). Magnetisation measurements were performed with a VSM on a Quantum Design PPMS-9T. Magnetometry data above $T = 400$ K were collected using the Quantum Design VSM oven option. Magnetic entropy changes were calculated from the isothermal magnetisation curves data using Maxwell relations [18]. Thermal expansion measurements were performed using a capacitance dilatometer installed in the PPMS [19].

3. Results

X-ray diffraction data at room temperature confirmed the correct antiperovskite phase with $Pm-3m$ symmetry is formed for both A = Ni and Sn

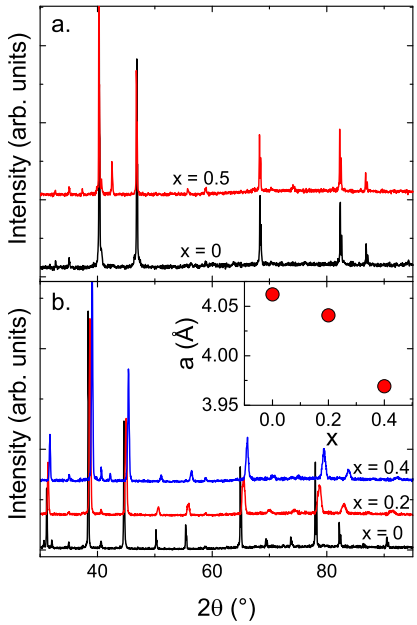

Figure 2: X-ray diffraction data for **a.** $Mn_{3+x}Ni_{1-x}N$ and **b.** $Mn_{3+x}Sn_{1-x}N$ samples. The inset for **b.** shows the refined lattice parameter, a, for the three $Mn_{3+x}Sn_{1-x}N$ samples.

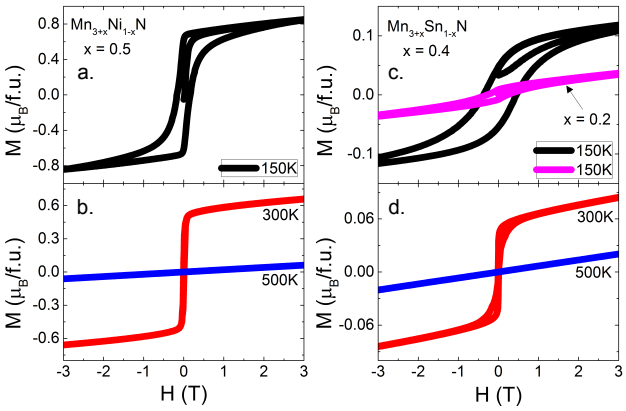

Figure 3: Isothermal magnetisation loops collected at the indicated temperatures for **a - b.** $Mn_{3.5}Ni_{0.5}N$ ($x = 0.5$), and **c - d.** $Mn_{3.4}Sn_{0.6}N$ ($x = 0.4$). Figure **c.** also shows $Mn_{3.2}Sn_{0.8}N$ ($x = 0.2$) at $T = 150\,\mathrm{K}$ for comparison.

(Figure 2). For A = Ni the refined lattice parameter for $x = 0$ ($a = 3.8870\,\text{Å}$) agree with literature data ($a = 3.8868\,\text{Å}$ [3]), whilst for $x = 0.5$ the lattice parameter increases ($a = 3.8908\,\text{Å}$), again as expected. For A = Sn, the lattice parameter for the $x = 0$ sample ($a = 4.0619\,\text{Å}$) agrees with reported data ($a = 4.06\,\text{Å}$[9]). As x increases the lattice shrinks significantly ($a_{x=0.4} = 3.9692\,\text{Å}$), which is expected due to the smaller metallic radius of Mn (127 pm) compared to Sn (163 pm) [20] and that $a = 3.872\,\text{Å}$ for Mn_4N [14].

Magnetisation measurements on the $x = 0$ end-members for both A = Ni and Sn have been reported previously [11, 13] and our data closely agree. For A = Ni and Sn the materials undergo a paramagnetic (PM) to antiferromagnetic (AFM) transition at $T_N = 262\,\mathrm{K}$ and 475 K respectively, whilst for the latter several further transitions between AFM states occur as a function of temperature as indicated in Figure 1b. Samples with $x > 0$ show quite different magnetic behaviour as expected with Mn doping. For $Mn_{3.5}Ni_{0.5}N$ the magnetic phase diagram is defined by two clear transitions: a PM to FM-like transition at $T_C \sim 480\,\mathrm{K}$ and an AFM-like transition at $T_N \sim 210\,\mathrm{K}$, in good agreement with the literature [12]. For $Mn_{3.2}Sn_{0.8}N$ and $Mn_{3.4}Sn_{0.6}N$, two clear transitions are also present: a PM to FM-like at $T_C = 390$ and 450 K, respectively, and an AFM-like at $T_N \sim 300\,\mathrm{K}$ for both samples. In both families the magnetisation is several orders of magnitude larger than for the $x = 0$ end-members (Figure 3). For $Mn_{3+x}Ni_{1-x}N$ the magnetic structure at $x > 0$ is a combination of FM on the Mn_p sites and Γ_{5g} AFM on the Mn_f sites [3] - thus it is considered a two sublattice ferrimagnetic (FIM) structure, as is found in the $x = 1$, Mn_4N end-member [21]. From the similar magnetic behaviour in the A = Sn family in Figure 3, a related magnetic structure can be inferred. Whilst AFM-like transitions occur in the high magnetisation states of all our $x > 0$ samples, calculation of the peak magnetic entropy change for $0 - 2\,\mathrm{T}$, ΔS_M, across T_N using Maxwells relation [18] gave unimpressive values of $0.6\,\mathrm{J\,Kg^{-1}\,K^{-1}}$ and $0.12\,\mathrm{J\,Kg^{-1}\,K^{-1}}$ for $Mn_{3.5}Ni_{0.5}N$ and $Mn_{3.4}Sn_{0.6}N$, respectively.

The temperature dependence of the isothermal magnetisation loops is quite similar for both Ni and Sn families (Figure 3). Below T_C a soft FM-like $M(H)$ loop occurs with negligible hysteresis although incomplete saturation even at $H = 3\,\mathrm{T}$ suggests ferrimagnetic behaviour. Below T_N, the shape of the $M(H)$ loops remain almost identical although large hysteretic behaviour is introduced, which for A = Sn increases systematically with increasing x. For $Mn_{3.5}Ni_{0.5}N$ and $Mn_{3.4}Sn_{0.6}N$, this hysteresis can be characterised by coercive fields of $H_C = 0.15\,\mathrm{T}$ and 0.37 T, respectively. Such hysteretic behaviour is not found in Mn_4N ($H_C = 0.0017\,\mathrm{T}$) [22], which has a collinear FIM structure

with a large $Mn_p = 3.8\,\mu B$ moment and an antiparallel $Mn_f = 0.9\,\mu_B$ moment [14]. Thus, the behaviour in our samples suggests additional magnetic complexity compared to the simple FIM of the $x = 1$ end-member, such as increased magnetocrystalline anisotropy.

The magnetisation as a function of temperature under different fields measured on our samples is shown in Figure 4. Both the A = Ni, $x = 0.5$ and A = Sn, $x = 0.4$ samples display negative magnetisation when measured under zero-field-cooled (ZFC) conditions below the Néel temperature. Negative magnetisation under ZFC conditions is often attributed to extrinsic effects such as negative trapped flux in superconducting magnets [23] and in fact there are very few instances in the literature of true negative magnetisation under such conditions. We confirmed that trapped flux is not the cause of negative magnetisation in our samples by following the procedure detailed by Kumar *et al.* for removing remnant fields [24]. As such, all magnetisation measurements shown in Figure 4 were performed after approaching zero field by oscillating from positive to negative with the final field set to be positive.

As mentioned, negative magnetisation under only ZFC conditions is rare. In one of the few examples we found in the literature, the ternary metallic alloy UPdSb shows negative magnetisation in ZFC measurements at temperatures well below its $T_C = 77\,K$ [25]. In this material it is assigned to strong magnetocrystalline anisotropy compared to the exchange energy, although the exact mechanism remains unclear. In fact, it is thought that a finite magnetic anisotropy is essential for the appearance of negative magnetisation in addition to two or more magnetically coupled sublattices [24]. Without the former only magnetic compensation occurs as in a typical FIM, such as Mn_4N. Therefore, the appearance of negative magnetisation in $Mn_{3+x}A_{1-x}N$ is further evidence that the magnetic structure has additional complexity and, additionally, it indicates that magnetic anisotropy is present. Other related antiperovskite carbides are reported to have high magnetic anisotropy, so this conjecture is consistent with this. The hysteretic behaviour of the $M(H)$ loops, seen in Figure 3, which opens below T_N *i.e.* at the point where negative magnetisation occurs, may be attributed to finite magnetocrystalline anisotropy. Comparing the two families, A = Ni and Sn, the former has a smaller compensation field for switching the magnetisation polarity of between $0.01 < H < 0.05\,T$, whilst the latter is $0.2 < H < 0.3\,T$. This behavior correlates with the larger coercive field in the A = Sn family and therefore larger magnetocrystalline anisotropy.

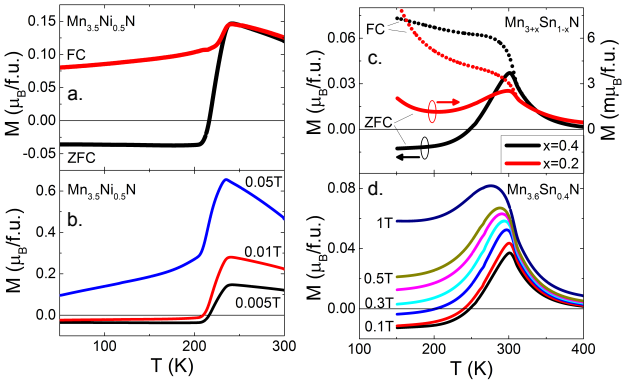

Figure 4: Magnetometry data collected on **a - b.** $Mn_{3.5}Ni_{0.5}N$ and **c - d.** $Mn_{3.6}Sn_{0.4}N$. Measurements taken under ZFC conditions were performed after treating for remnant fields above T_N. For each compound, A = Ni or Sn, the top figure shows that the negative magnetisation is only present under ZFC conditions, whilst the bottom figure shows how the negative magnetisation disappears under increasingly large measuring fields.

Whilst negative magnetisation materials are interesting in their own right, for instance due the bi-polar magnetic entropy change [24], for the $Mn_{3+x}A_{1-x}N$ family the phenomenon may have relevance to their other properties, such as the phenomena of near-ZTE immediately below T_N. This effect evidently requires MVC however it is composition dependent and not fully understood. In $Mn_{3+x}Ni_{1-x}N$, doping Mn onto the Ni site causes broadening of the sharp volume change at T_N and induces a region of near-ZTE immediately below [3]. It is argued that stabilisation of the Γ_{5g} magnetic structure underlies the near-ZTE in this material. Similar near-ZTE behaviour below T_N is induced in $Mn_3Cu_{1-x}Sn_xN$ and $Mn_3Cu_{1-x}Ge_xN$, neither of which possess the Γ_{5g} magnetic structure, however in the opposite sense to $Mn_{3+x}Ni_{1-x}N$: the near-ZTE region appears only when the volume change at T_N is sharp [13, 26, 27]. Taken together this suggests that *additional contributions* to the thermal expansion below T_N are required for the near-ZTE in these antiperovskites.

Thermal expansion can be determined using dilatometry measurements, which we have performed on our samples. For Mn_3SnN and $Mn_{3.2}Sn_{0.8}N$ ($T_N = 300\,K$), the MVC is negligible and therefore no features appear in the linear ther-

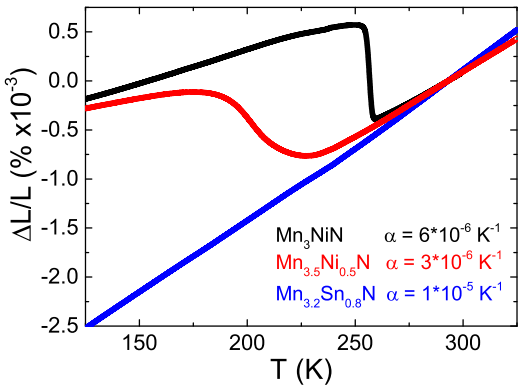

Figure 5: Dilatometry data collected on Mn_3NiN, $Mn_{3.5}Ni_{0.5}N$ and $Mn_{3.2}Sn_{0.8}N$. Thermal expansion coefficients, α, were fitted between $125 < T(\mathrm{K}) < 175$.

mal expansion at T_N and the thermal expansion coefficient $\alpha = 1 \times 10^{-5}\,\mathrm{K}^{-1}$ is a normal value, as can been seen in Figure 5. For $Mn_{3+x}Ni_{1-x}N$ with MVC the large volume change at T_N broadens as x increases and α below T_N halves from 6×10^{-6} to $3 \times 10^{-6}\,\mathrm{K}^{-1}$, in agreement with previous findings by Deng *et al.* [3]. We now compare these results with those from the A = Ag and Ga members of the $Mn_{3+x}A_{1-x}N$ family. Similar broadening of the large volume change at T_N occurs with Mn doping for both A = Ag and Ga [16, 17], where both compositions possess the Γ_{5g} magnetic structure. Moreover, for large values of x for A = Ag α below T_N reduces to $1.7 \times 10^{-6}\,\mathrm{K}^{-1}$ and coincides with increased competition between AFM and FM magnetic phases [16]. Large values of x were not measured for A = Ga, nor was α below T_N, however the broadening behaviour up to $x = 0.3$ is similar [17]. The observation that Mn doping in the A = Ag, Ga and Ni families, where the $x = 0$ members have MVC and the Γ_{5g} magnetic structure, leads to near-ZTE behaviour below T_N indicates that a sizeable magnetic moment on the A site is required for this phenomenon. Thus we summise that, alongside MVC and the Γ_{5g} structure, the competing sublattices and magnetocrystalline anisotropy, which are essential components required for the creation of the negative magnetisation in our A = Ni, $x = 0.5$ samples, also influence the near-ZTE at intermediate temperatures below T_N in these antiperovskites.

4. Conclusions

In conclusion, we have explored the effect of excess Mn doping in the manganese antiperovskite family $Mn_{3+x}A_{1-x}N$ for A = Ni and Sn as a function of x. We find that with increased Mn doping additional magnetic phases are introduced with competing sublattices, previously unreported for A = Sn. For $Mn_{3.5}Ni_{0.5}N$ and $Mn_{3.6}Sn_{0.4}N$ we find a rare case of negative magnetisation below T_N, a phenomenon that requires both coupled sublattices and magnetocrystalline anisotropy. We propose that the latter two properties, combined with MVC, influence the near-ZTE at intermediate temperatures below T_N in the A = Ni family. We plan to further study the underlying mechanism of the negative magnetisation using neutron diffraction, which will also elucidate the magnetic structure phase diagram for A = Sn below $x < 0.5$.

5. Acknowledgements

This work was supported by the European Community 7th Framework Programme (Grant number 310748, DRREAM) and the EPSRC (Grant EP/K503733/1).

References

[1] K. Takenaka, Negative thermal expansion materials: technological key for control of thermal expansion, Science and Technology of Advanced Materials 13 (2012) 013001.

[2] E. O. Chi, W. S. Kim, N. H. Hur, Nearly zero temperature coefficient of resistivity in antiperovskite compound CuNMn3, Solid State Communications 120 (2001) 307–310.

[3] S. Deng, Y. Sun, H. Wu, Q. Huang, J. Yan, K. Shi, M. I. Malik, H. Lu, L. Wang, R. Huang, L. Li, C. Wang, Invar-like Behavior of Antiperovskite Mn 3+ x Ni 1 x N Compounds, Chemistry of Materials 27 (2015) 2495–2501.

[4] K. Shi, Y. Sun, J. Yan, S. Deng, L. Wang, H. Wu, P. Hu, H. Lu, M. I. Malik, Q. Huang, C. Wang, Baromagnetic Effect in Antiperovskite Mn3Ga0.95N0.94 by Neutron Powder Diffraction Analysis, Advanced Materials 28 (2016) 3761–3767.

[5] J. Zemen, Z. Gercsi, K. G. Sandeman, Piezomagnetic effect as a counterpart of negative thermal expansion in magnetically frustrated Mn-based antiperovskite nitrides, arXiv 1512.03470 (2015) 1–8.

[6] D. Matsunami, A. Fujita, K. Takenaka, M. Kano, Giant barocaloric effect enhanced by the frustration of the antiferromagnetic phase in Mn3GaN, Nature materials 14 (2015) 73–8.

[7] J.-P. Jardin, J. Labbe, Phase transitions and band structure in metallic perovskites (carbides and nitrides), Journal of Solid State Chemistry 46 (1983) 275–293.

[8] E. Bertaut, D. Fruchart, J. Bouchaud, R. Fruchart, Diffraction neutronique de Mn3GaN, Solid State Communications 6 (1968) 251–256.

[9] M. R. Fruchart, R. Madar, M. Barberon, E. Fruchart, M. G. Lorthioir, Transitions magnétiques et déformations cristallographiques associées dans les nitrures du type perowskite ZnMn3N et SnMn3N, J. Phys. Colloques 32 (1971) 982–984.

[10] D. Fruchart, E. Bertaut, J. Senateur, R. Fruchart, Magnetic studies on the metallic perovskite-type compound Mn 3SnN, J. Physique Lett. 38 (1977) 21–23.

[11] D. Fruchart, E. F. Bertaut, Magnetic Studies of the Metallic Perovskite-Type Compounds of Manganese, Journal of the Physical Society of Japan 44 (1978) 781–791.

[12] P. L'Héritier, D. Fruchart, R. Madar, R. Fruchart, 1.5.6 Metallic Perovskites: Datasheet from Landolt-Börnstein - Group III Condensed Matter - Volume 19C, ???? doi:10.1007/10353201{_}70.

[13] K. Takenaka, M. Ichigo, T. Hamada, A. Ozawa, T. Shibayama, T. Inagaki, K. Asano, Magnetovolume effects in manganese nitrides with antiperovskite structure, Science and Technology of Advanced Materials 15 (2014) 015009.

[14] M. Mekata, Magnetic study on Mn4N and its related compounds, Journal of the Physical Society of Japan 17 (1962) 796–803.

[15] W. Feng, D. Li, W. Ren, Y. Li, W. Li, J. Li, Y. Zhang, Z. Zhang, Structural, magnetic and transport properties of Mn3.1Sn0.9 and Mn3.1Sn0.9N compounds, Journal of Alloys and Compounds 437 (2007) 27–33.

[16] J. C. Lin, P. Tong, W. Tong, S. Lin, B. S. Wang, W. H. Song, Y. M. Zou, Y. P. Sun, Tunable negative thermal expansion related with the gradual evolution of antiferromagnetic ordering in antiperovskite manganese nitrides Ag1-xNMn3+x (0 ¡ x ¡ 0.6), Applied Physics Letters 106 (2015) 3–8.

[17] X. G. Guo, J. C. Lin, P. Tong, M. Wang, Y. Wu, C. Yang, B. Song, S. Lin, W. H. Song, Y. P. Sun, Magnetically driven negative thermal expansion in antiperovskite, Applied Physics Letters 107 (2015) 202406.

[18] A. M. Tishin, Y. I. Spichkin, The magnetocaloric effect and its applications, Institue of Physics Publishing, Bristol and Philadelphia, 2003.

[19] M. Rotter, H. Müller, E. Gratz, M. Doerr, M. Loewenhaupt, A miniature capacitance dilatometer for thermal expansion and magnetostriction, Review of Scientific Instruments 69 (1998) 2742–2746.

[20] G. W. C. Kaye, T. H. Laby, Tables of physical and chemical constants, 15 ed., Longman, London, UK, 1993.

[21] W. Takei, R. Heikes, G. Shirane, Magnetic Structure of Mn4N type compounds, Physical review 810 (1962).

[22] C. Li, Y. Yang, L. Lv, H. Huang, Z. Wang, S. Yang, Fabrication and magnetic characteristic of ferrimagnetic bulk Mn4N, Journal of Alloys and Compounds 457 (2008) 57–60.

[23] N. Kumar, a. Sundaresan, On the observation of negative magnetization under zero-field-cooled process, Solid State Communications 150 (2010) 1162–1164.

[24] A. Kumar, S. Yusuf, The phenomenon of negative magnetization and its implications, Physics Reports 556 (2015) 1–34.

[25] K. Gofryk, D. Kaczorowski, On the magnetic and electrical behaviour of UPdSb, Journal of Physics Condensed Matter 18 (2006) 3887–3896.

[26] K. Takenaka, H. Takagi, Magnetovolume Effect and Negative Thermal Expansion in Mn3(Cu1-xGex)N, Materials Transactions 47 (2006) 471–474.

[27] K. Takenaka, H. Takagi, Giant negative thermal expansion in Ge-doped anti-perovskite manganese nitrides, Applied Physics Letters 87 (2005) 261902.